Biophysical Characterization of Chromatin Remodeling Protein CHD4

Rosa Morra, Tomas Fessl, Yuchong Wang, Erika J. Mancini, and Roman Tuma

Abstract

Chromatin-remodeling ATPases modulate histones–DNA interactions within nucleosomes and regulate transcription. At the heart of remodeling, ATPase is a helicase-like motor flanked by a variety of conserved targeting domains. CHD4 is the core subunit of the nucleosome remodeling and deacetylase complex NuRD and harbors tandem plant homeo finger (tPHD) and chromo (tCHD) domains. We describe a multifaceted approach to link the domain structure with function, using quantitative assays for DNA and histone binding, ATPase activity, shape reconstruction from solution scattering data, and single molecule translocation assays. These approaches are complementary to high-resolution structure determination.

Key words Nucleosome, ATPase, Surface plasmon resonance, SAXS, TIRF, FRET

1 Introduction

Chromodomain helicase DNA-binding protein 4 (CHD4), which is sometimes referred to as Mi2β, is an SNF2-type chromatin remodeling motor [1] and the main subunit of the nucleosome remodeling and deacetylase (NuRD) [2–5]. The complex is involved in gene transcription regulation [6, 7] by mediating histone deacetylation. Unlike other remodelers, such as SWI/SNF, NuRD is thought to act as a transcriptional repressor [8] and achieves its function through the combination of a motor protein, CHD4, with other subunits such as the histone deacetylases HDAC1 and HDAC2 [6]. The key questions for any remodeling motor are how the ATPase is targeted to specific sites within the chromatin environment and how ATP hydrolysis is coupled to the remodeling activity. In order to answer these questions, it is important to dissect the domain structure and function of the protein.

In addition to the ATPase domain, CHD4 harbors two plant zinc finger homeodomains arranged in a tandem fashion (tPHD). These are common in nucleosome/histone-binding proteins

[9–11]. It also exhibits tandem chromodomains (tCHD) which have been shown to mediate chromatin interaction by binding directly to either DNA, RNA, or methylated histone H3 [12–15]. The combination of tPHD and tCHD is specific for the CHD family (CHD3, CHD4, and CHD5) [16], however simultaneous presence of several histone-binding modules is prevalent for many chromatin remodeling ATPases.

Here we describe biochemical and biophysical methods which were instrumental in shedding light on the mechanism by which these domains cooperate in the context of ATPase-driven nucleosome remodeling [17]. We describe cloning and purification of the individual tandem domains and various ATPase constructs and characterize their binding to nucleic acids and various modified histone tails using electrophoretic mobility shift assay (EMSA) and surface plasmon resonance (SPR), respectively. ATPase assay is used to demonstrate cooperation between the tPHD and tCHD domains and the ATPase module. We describe a novel single molecule assay to visualize CHD4 translocation along DNA.

2 Materials

2.1 Cloning and Expression

pTriEx2 vector (Novagen).

BL21 (DE3) supercompetent cells (Agilent).

XL1 supercompetent cells (Agilent).

DNA using miniprep kit (Qiagen).

1 M stock of isopropyl-thiogalactopyranoside (IPTG, Sigma).

Lysogeny broth (LB): 10 g bacto-tryptone, 5 g yeast extract, 10 g NaCl per 1 L media.

Terrific broth (TB): 12 g bacto-tryptone, 24 g yeast extract, 4 mL glycerol per 1 L media.

2.2 Protein Purification

Lysis buffer: 50 mM sodium phosphate pH 7.5, 500 mM NaCl, 5 mM imidazole, 0.2 % Tween 20, protease inhibitor cocktail tablet (Roche).

Talon™ resin (Clontech).

Imidazole (Sigma).

HiTrap Chelating column 5 mL (GE Healthcare).

Superdex S200 10/30 (GE Healthcare).

S75 10/30 column (GE Heathcare).

SEC buffer: 20 mM Tris pH 7.5, 200 mM NaCl, 1 mM DTT.

Acryl amide 30 % stock (Severn Biotec).

2.3 Nucleic Acid-Binding EMSA	MW marker Gene Ruler 100 bp Plus DNA ladder (Fermentas).
	MW marker XIII 50-750 (Roche).
	MW marker Gene Ruler 1 Kb and 100 bp Plus DNA ladder (Invitrogen).
	Molecular biology grade agarose (Sigma).
	DNA-binding buffer: 20 mM Tris pH 7.5, 200 mM NaCl.
	TAE buffer: prepared from 10× TAE stock: 48.4 g Tris base, 11.4 mL glacial acetic acid, 3.7 g EDTA disodium salt per 1 L.
	Ethidium bromide 1000× stock: 10 mg/mL.
2.4 ATPase Assay	EnzChek phosphate release assay (Life Technologies/Thermo-Fisher).
	100 mM ATP stock solution, pH 7 (Jena Biosciences).
	10× standard buffer: 400 mM Tris pH 7.5, 500 mM NaCl, 50 mM $MgCl_2$.
2.5 NCP Mobility Shift	NCP-binding buffer: 20 Tris–HCl pH 8, 200 mM NaCl, 10% sucrose.
	λ-DNA (Stratagene).
	Acryl amide 30% stock (Severn Biotec).
	10% glycerol.
	Native running buffer: 20 mM Hepes pH 8, 1 mM EDTA.
2.6 SPR	Streptavidin sensor chips (GE Healthcare).
	0.05 M Sodium hydroxide activation and regeneration solution (GE Healthcare).
	SPR buffer: 20 mM Tris pH 7.5, 200 mM NaCl, 0.05% (v/v) polysorbate 20 (GE Healthcare).
	Biotinylated and differentially methylated (at Lys4 and Lys9) histone H3 peptides were custom synthesized by Millipore.
	Wash solution 1: 0.05% SDS.
	Wash solution 2: 0.9 M NaCl.
	100 mM ATP stock solution, pH 7 (Jena Biosciences).
2.7 Labeling of Protein and DNA with Fluorescent Dyes	Plasmid pGEM-3z/601 (Addgene plasmid 26656).
	Alexa Fluor 594 maleimide (Life Technologies/Thermo-Fisher).
	Alexa Fluor 488-labeled forward primer (Life Technologies/Thermo-Fisher):
	5′-AF 488-GCCCTGGAGAATCCCGGTGC-3′.
	Biotinylated reverse:
	5′-Biotin-CAGGTCGGGAGCTCGGAACACTATC-3′.

PCR kit (Promega).

SYBR Gold stain (Life Technologies/Thermo-Fisher).

BamHI restriction enzyme (New England Biolabs).

HindIII restriction enzyme (New England Biolabs).

Labeling reaction buffer: 20 mM Tris pH 7.5, 200 mM NaCl.

Dialysis buffer: 20 mM Tris pH 7.5, 200 mM NaCl, 1 mM DTT.

Molecular biology grade agarose (Sigma).

LB Amp agar plates.

2× TY-AC medium: 16 g bacto-tryptone, 10 g yeast extract, 5 g NaCl.

Ampicillin (Amp) 1000× stock solution 100 mg/mL.

2.8 Single Molecule Fluorescence Imaging

Glass cover slips (Thermo-Fisher).

Vectabond reagent (Vector Laboratories, Burlingame, USA).

Polyethyleneglycol succinimidyl ester (PEG-NHS, Rapp Polymere).

Biotinylated-PEG-NHS (Rapp Polymere).

0.1 M sodium bicarbonate buffer, pH 8.3 (SigmaUltra).

10 mM Tris, pH 7.4 (SigmaUltra).

Immunopure-streptavidin (Pierce Biotechnology).

Buffer A: 25 mM Tris acetate, pH 8.0 with 8 mM magnesium acetate (SigmaUltra), 100 mM KCl, 1 mM dithiothreitol, and 3.5% (w/v) poly-ethylene glycol 6000 (SigmaUltra).

Anti-photobleaching cocktail; 1.25 mM propyl gallate, 5 mM DTT, 5 mM cysteamine, 1.5 mM β-mercaptoethanol (Fluka/SigmaAldrich).
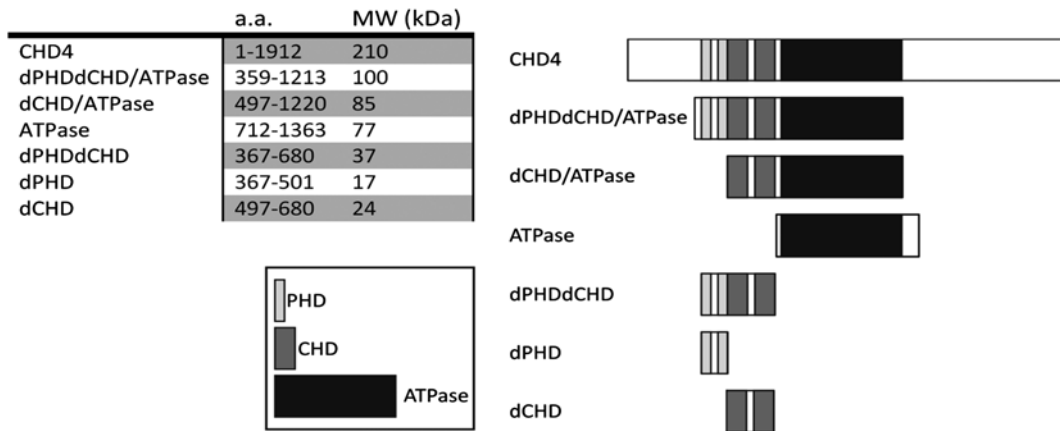
3 Methods

3.1 Expression and Purification of CHD4 Constructs

The cloning and purification method is rather generic and is used for all the constructs generated here. However, it might need to be modified for different chromatin remodeling ATPases, which, as many nuclear proteins, are known to have solubility problems. For example it may not be possible to obtain the full-length protein in a soluble, active form and a suitable truncation will need to be devised, as shown here for CHD4 (Fig. 1).

1. Select domains based on predicted gene structure (GeneBank, Fig. 1). Generate C-terminal 8xHis-tagged construct by PCR using human CHD4 cDNA (Mammalian Gene Collection) as a template and appropriate sets of primers containing cloning sites compatible with the recipient plasmid (*see* **Note 1**).

	a.a.	MW (kDa)
CHD4	1–1912	210
dPHDdCHD/ATPase	359–1213	100
dCHD/ATPase	497–1220	85
ATPase	712–1363	77
dPHDdCHD	367–680	37
dPHD	367–501	17
dCHD	497–680	24

Fig. 1 Domain constructs used in this study, relative molecular weights (*left*) and position within the full-length CHD4 (*right*)

2. Ligate the amplified PCR product into the expression vector (in this case pTriEx2) and transform XL1 cells using appropriate antibiotic (Amp) for selection.

3. Select colonies, grow overnight culture, and extract plasmid DNA using miniprep kit (Qiagen). Verify insert by sequencing.

4. Transform *E. coli* BL21 (DE3) supercompetent expression cells.

5. Select colonies and inoculate an overnight booster LB culture (100 mL).

6. Inoculate 6×0.5 L of TB with 10 mL of the booster and grow at 37 °C till $OD_{600} = 0.6$.

7. Chill to below 20 °C on ice or in cold room and induce with 0.7 mM IPTG (final concentration).

8. Grow culture overnight at 20 °C shaking (225 rpm).

9. Harvest cells by centrifugation at $3500 \times g$ for 15 min at 4 °C.

10. Resuspend cell pellets in 30 mL of the lysis buffer and lyse the cells using a French pressure cell (Aminco).

11. Clarify the lysate by centrifugation at $15,3446 \times g$ (SW32Ti rotor) for 1 h, 4 °C.

12. Collect supernatant and mix with Talon™ resin.

13. Elute with an imidazole gradient and check protein composition in fractions by 12 % SDS-PAGE (10 μL samples mixed with 20 μL of 2× sample-loading buffer).

14. Inject up to 5 mL of the collected fractions onto S-200 (25/300) column and elute with flow rate 3 mL/min at room temperature.

15. Run SDS-PAGE gel on fractions and check the purity and integrity of proteins by mass spectrometry (*see* **Note 2**).

16. Determine the protein concentration using predicted extinction coefficient.

3.2 Multiple Angle Light Scattering (MALS)

MALS gives estimate of the native mass and thus can inform of the oligomeric status or non-covalent association between subunits or domains.

1. Configure the light-scattering instrumentation (DAWN HELEOS II, Wyatt Technology, Santa Barbara, CA) in a flow cell mode coupled to an analytical Superdex S200 or S75 10/300 column (flow rate 0.5 mL/min).

2. Line up a differential refractive index (RI, Optilab rEX, Wyatt Technology) and Agilent 1200 UV (Agilent Technologies) detectors after the exit from the light-scattering flow cell. If necessary adjust sensitivity of RI and UV/VIS detectors (*see* **Note 3**). Some light-scattering instruments allow adjusting the laser power, i.e. higher power for samples with low concentration (*see* **Note 4**).

3. Equilibrate the column in the desired buffer, flush the reference cell of the RI detector and zero both RI and UV/VIS detectors.

4. Inject 0.1–0.5 mL of BSA standard sample (*see* **Note 5**) (~2 mg/mL; *see* **Note 6**) and collect data for the duration of the HPLC run. This data will be used to calibrate the light-scattering detector. Analyze the data to determine the calibration constant.

5. Analyzed the data using the software provided with the instrument (ASTRA software package, Wyatt Technology). For the analysis you will need to specify the calibration constant (obtained in 3 above), temperature, an estimated dn/dc (refractive index increment, typical value 0.15) and/or molar extinction coefficient predicted from amino acid composition (http://web.expasy.org/protparam/).

3.3 Multiplexed DNA-Binding Assay

Electrophoretic gel mobility shift assays constitute a standard method to detect formation of stable nucleic acid protein complexes. Usually, these are done using a single-labeled probe with a defined length. However, chromatin remodeling complexes, which often have multiple DNA-binding domains, may discriminate between short and longer DNAs. Hence, it is desirable to probe association with multiple DNA fragments of various lengths. A simple way to implement this is to use a generic ladder DNA (Fig. 2). However, this approach is qualitative and, due to overlap of shifted bands, may not allow determination of dissociation constants.
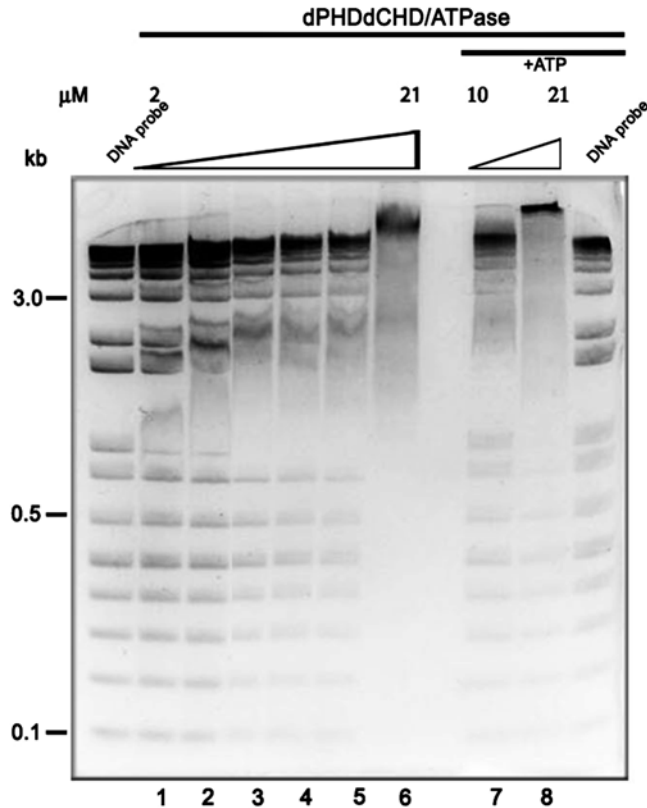
Fig. 2 Multiplexed variable length EMSA. Agarose gel image of ladder DNA in the absence (DNA probe) and presence of increasing concentration of CHD4 construct (*lanes 1–6*) and in the presence of 1 mM ATP (*lanes 7–8*)

1. Mix dsDNA MW marker (*see* **Note 7**) probe with increasing amounts of CHD4 (*see* **Note 8**) constructs in 20 μL of DNA-binding buffer and incubate for 5 min at room temperature (or any desired temperature).

2. Add 2 μL of loading buffer and load the sample onto a 2% agarose gel.

3. Run the gel in 1× TAE buffer at 20 mA for 40 min.

4. Stained for 10 min with 1× ethidium bromide and visualize DNA–protein complexes by UV light with long-pass filter.

5. If the bands are well resolved, quantification of the shifts can be attempted using imaging and analysis software.

3.4 Nucleosome Core Particle Mobility Shift Assay

Preparation of histones and reconstitution of nucleosomes (NC) is an art of its own and is beyond the scope of this chapter. We refer the reader to recent and classic publications on histone production [18, 19] and nucleosome core particle (NCP) reconstitution [20]. Only steps pertaining to the NC mobility shift assay are delineated below (*see* **Note 9**).

1. Reconstitute NCP (50 fmol) with radiolabeled (or fluorescently labeled) DNA (168 bp PCR fragment) by salt gradient dialysis [21].

2. Incubate with increasing amount of CHD4 construct for 15 min on ice in 10 μL of NCP-binding buffer.

3. For the chasing control experiment (*see* **Note 10**), after the incubation on ice, add 200× excess (by weight) of λ-DNA and incubate on ice for a further 10 min.

4. Run a native gel electrophoresis (5 % polyacrylamide) containing 10 % glycerol in the native running buffer at 15 mA for 3 h.

5. Visualize the gel by phosphorimager or autoradiography.

3.5 SPR Histone Tail Binding Studies

SPR is one of the most popular techniques to follow binding kinetics in vitro. It offers multiplexing and high-throughput in a fully automated format. Perhaps the only drawback is the requirement to immobilize one of the binding partners. Since the technique relies on the changes in refractive index close to the probed surface it is common that the smaller of the binding partners (ligand) is immobilized while the larger entity (receptor) is flown over the surface in order to produce large signal changes (*see* **Note 11**). Our SPR binding studies were performed using a Biacore 2000/3000 and T100 (GE Healthcare) at 25 °C in SPR buffer.

1. Check protein concentrations (*see* **Note 12**) by measuring absorbance at 280 nm using calculated molar extinction coefficients.

2. Unpack and insert the sensor and activate the surface with streptavidin following the manufacturer's recommendation (*see* **Note 13**).

3. Immobilize biotinylated histone peptides onto the sensor chip following manufacturer's instructions. Relatively low histone peptide immobilization levels (40–90 resonance units (*see* **Note 14**)) are desirable to minimize mass transport artifacts [22]. Prepare the surfaces of the three flow cells (Fc2, Fc3, Fc4) (*see* **Note 15**) and separately immobilize different peptides (flow rate of 20 μL/min) using Fc1 as the reference cell to gauge surface density (*see* **Note 16**).

4. Flow different concentrations of CHD4 construct through all chambers on the chip using a fast flow rate of 100 μL/min (*see* **Note 17**).

5. Between individual injections regenerate the chip by three repeated application of 0.05 % SDS followed by a 0.9 M NaCl wash and then equilibrate in the binding buffer.

6. Repeat all measurements at least three times.

7. The signal from experimental flow cells is then corrected by subtraction of reference signal (flow cell Fc1).

8. When appropriate, the data can be globally fitted with a second-order association reaction model (approximated by a pseudo-first-order reaction with rate constant $k = k_{on}[\text{ligand}]$ for each ligand concentration) followed by a first-order dissociation with characteristic kinetic constants k_{on} and k_{off} (Fig 3b) (*see* **Note 18**).

9. In the case of fast binding/unbinding kinetics (Fig. 3a) the equilibrium dissociation constants K_d values can be obtained from the steady-state plateau values. These are simply fit to Langmuir binding isotherm (bound = $C*\text{max}/(K_d + C)$, where C is analyte concentration and max is the saturation level, Fig. 3c).

10. Add ATP (1 mM final concentration) to the protein before injection onto the sensor chip to probe affinity modulation by ATPase domain (*see* **Note 19**).

3.6 ATPase Activity Assay

There are many ATPase assays available on the market. We have selected the EnzCheck (Thermo-Fisher) inorganic phosphate (P_i) release assay, which is a quantitative spectrophotometric assay based on coupled enzymatic reaction and chromogenic substrate. This assay supports steady-state kinetic measurements in real time without the need to quench and measure individual time points. The adaptation of the assay to a 96-well plate (*see* **Note 20**) is particularly useful for determination of kinetic parameters (k_{cat}, the turnover number; K_M, Michaelis constant) [23].

1. Calculate the mixing volumes for the desired conditions for each well. Use an optically transparent, flat bottom, 96-well plate.

2. Dilute the standard 10× buffer by adding 20 μL for 200 μL final volume per well, add 40 μL of MESG chromogenic substrate, 2 μL PnPase enzyme, suitable ATPase aliquot (final concentration 0.1 to 1 μM, depending on the expected activity). Add deionized water to top up to final volume (*see* **Note 21**).

3. Aliquot inorganic phosphate KH_2PO_4 standards (0, 20, 40, 60, and 100 μM final concentration) into positive control wells (*see* **Note 22**).

4. Mix wells and insert the plate into the plate reader equipped with absorption filter at 360 nm (or a monochromator tuned to that wavelength) and collect 5 min baseline read. Depending on number of wells read and the type of the plate, reader set the data collection to record each well at least every 30 s (*see* **Note 23**).
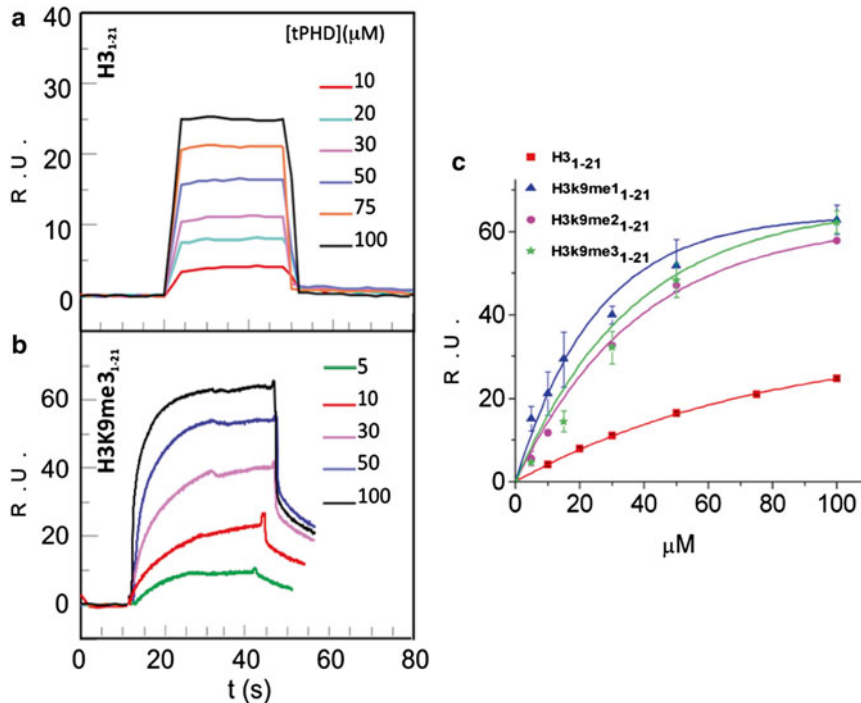
Fig. 3 SPR binding of tandem PHD domains to surface immobilized H3 unmethylated (**a**) and K9 trimethylated peptides (**b**) and the resulting Langmuir isotherm for equilibrium binding (**c**)

5. Add ATP alone without the ATPase as a background control (*see* **Note 24**). Another negative control is the assay mix including the ATPase but without ATP to check for presence of inorganic phosphate in the protein sample (*see* **Note 25**).

6. Add ATP to achieve the desired concentrations in the ATPase samples, mix wells and insert the plate, and record absorbance changes at 360 nm for 20 min.

7. To estimate the ATPase turnover rate, the initial, linear portion of the raw data is fitted by linear regression (*see* **Note 26**) (using e.g. GraphPad Prism or Origin software) and the amount of P_i released per second is obtained from the slope of the regression line normalized by the molarity of protein (concentrations determined from absorbance at 280 nm using calculated molar extinction coefficients).

3.7 SAXS Data Collection and Processing

SAXS provides information on oligomeric status and overall shape of macromolecular assemblies. Here, we describe how it can be used to delineate the spatial disposition of different functional domains within a large protein. This requires successful expression of the individual domains in a folded and biologically active form. The latter is underpinned by the array of biochemical data, such as DNA- and histone tail-binding assays and ATPase activity as

discussed above. We only describe general sequence for data processing, leaving out much detail since that depends on the software package used. Our discourse is limited to the widely used ATSAS software package (http://www.embl-hamburg.de/biosaxs/software.html) developed by Dimtri Svergun and colleagues. Further technical intricacies of SAXS can be found in a recent excellent monograph [24].

1. Although SAXS data can be obtained on a modern laboratory X-ray source such a specialized equipment is not commonly found in labs and it is advisable to collect data at a synchrotron radiation facility such as ESRF (Grenoble, France), EMBL facility at the PETRA ring (Hamburg, Germany), or the Diamond Light Source (Harwell, U.K.). These facilities operate dedicated beamlines which are accessed via a rapid turnover proposal-based schemes. Collecting data for the work described here would need only one 8 h shift at present time. This might become even shorter with further automation of beamlines and remote access capacity.

2. This work employed ESRF beamline ID14-3 which uses a flow cell and automated sample loading system (*see* **Note 27**). A minimum of 10 μL of each sample is required to fill the scattering cell (*see* **Note 28**).

3. Confer with the beamline scientist to configure the system for the intended use, e.g. depending on the size of the complex and available amounts and concentrations.

4. Collect scattering from empty cell.

5. Collect scattering from water (*see* **Note 29**).

6. Collect scattering from buffer for the BSA standard (e.g. PBS).

7. Collect BSA standard of known concentration (2–5 g/L).

8. Each biomolecule sample is preceded and followed by collection of the matching buffer (*see* **Note 30**).

9. Ten or more successive frames (*see* **Note 31**) (10 s to 1 min duration) are collected and compared to check for radiation damage (*see* **Note 32**) and aggregation during each SAXS experiment.

10. The data are collected on 2D detectors and images are automatically integrated, averaged (*see* **Note 33**) and corrected to obtain 1D scattering intensities by the beamline software.

11. Further processing (manual background subtraction and averaging, data quality appraisal, Guinier plot) can be done with PRIMUS program package [25].

12. Draw the Guinier plot in PRIMUS to estimate molecular mass from the extrapolated intensity at zero angle (I_0) and radius of gyration (R_g) from the slope. Use BSA as standard (*see* **Note 34**) for estimating mass from I_0 (*see* **Note 35**).

13. Compute pair-wise distance distribution functions using indirect transformation method implemented in the GNOM program. The distribution is then used to estimate the maximum dimension ($D_{\max}$) [26, 27] and refine R_g.

14. Use the output file from GNOM as input for ab initio shape determination by programs DAMMIN [28] or DAMMIF [29] (*see* **Note 36**).

15. Superimpose models using the SUPCOMB program [30] and average them using DAMAVER [31].

16. Use DAMFILT to trim the model to the desired volume derived either from SAXS or from hydrodynamic and light-scattering experiments (R_h and mass) [31].

17. After obtaining models of individual domains attempt to fit the component structures into larger entities, e.g. tCHD and tPHD models into the tPHDtCHD model and tPHD, tCHD, and ATPase models into the tPHDtCHD/ATPase model. An initial model can be arrived at by visual docking in CHIMERA using volume overlap correlation [32].

18. Perform multiphase ab initio modeling using the program MONSA [28] in which three phases correspond to tPHD, tCHD, and ATPase domains and are either pre-assigned on the basis of the manual fitting or randomized (*see* **Note 37**).

3.8 Labeling CHD4 with Fluorescent Dye

CHD4 is an ATPase and is thought to be a molecular motor which can move along nucleic acids and reposition nucleosomes. In order to probe short range motion, CHD4 tPHDtCHD/ATPase was labeled with acceptor dye Alexa Fluor 590 maleimide. Maleimide reacts with cysteines accessible on CHD4 surface. Cysteine is chosen, since it is the least abundant amino acid in CHD4 (22 Cys) only few of them are expected to be exposed on the surface (*see* **Note 38**). All steps below are performed to limit exposure to intense light, e.g. wrapping tubes with aluminium foil or using dark tinted tubes.

1. Mix protein stock (10 μM) with 10-fold molar excess of Alexa Fluor dye (10 mM DMSO stock) and incubate for 8 h at 4 °C (*see* **Note 39**).

2. Dialyze labeled protein overnight and store in dark at 4 °C (*see* **Note 40**).

3. Determine the degree of labeling by recording UV/VIS absorbance spectrum of the conjugated protein and computing the protein concentration from absorbance at 280 nm corrected for the dye contribution estimated from abs. maximum of the dye at 590 nm. The correction factor is dye-specific and is listed in manufacturer manual (*see* **Note 41**) (0.56 for AF594). The molar ratio of label to protein should ideally be 1 or slightly higher (*see* **Note 42**).

4. Check the ATPase activity and DNA binding of the conjugated protein using assays described above.

3.9 Preparation of Labeled 601 Sequence

1. The pGEM-3z/601 with 601 sequence insert (Fig. 4a) was transformed into XL-1 *E. coli* cells and selected on LB Amp agar plates.

2. Pick a single colony and inoculate 15 mL 2× TY-AC Amp media, grow overnight.

3. Harvest cells and extract the plasmid using a miniprep kit.

4. Digested with BamHI and HindIII.

5. Separate on 2 % agarose gel.

6. Extract band corresponding to 601 sequence.

7. Use the extracted 601 sequence as template with Alexa Fluor 488 and biotin-labeled primers (Fig. 4b) and perform PCR: 50 μl of PCR reaction prepared by adding of 37 μL water, 1 μL plasmid template, 1 μL of both primers, and 10 μL of 5× pre-mixed PCR kit. PCR program: (5′ at 93 °C) and [(1′ at 93 °C and 1′ at 62 °C and 2′ at 72 °C)′ 30] and (10′ at 72 °C), product stored at 4 °C.

8. PCR product was separated on 2 % gel, excised and extracted by centrifugation and again purified on 2 % gel, stained with SYBR GOLD.

9. Check the degree of labeling and emission brightness of donor dye attached to DNA through recording UV/VIS absorption and fluorescence emission spectra.

3.10 DNA Immobilization

For TIRF imaging, DNA templates need to be immobilized onto a clean cover slip surface.

1. Prepare glass cover slip surfaces using the method presented by Rasnik and coworkers [33].

2. Incubate cover slips with Vectabond reagent according to the manufacturer instructions.

3. Coat with mixture of 25 % (w/v) PEG-NHS and 0.25 % (w/v) biotinylated-PEG-NHS in 0.1 M sodium bicarbonate (pH 8.3) for 3 h in order to eliminate non-specific adsorption of proteins.

4. Rinse with 10 mM Tris, pH 7.4 and incubate with 0.2 mg/mL Immunopure-streptavidin for 1 h then rinsed with 3 × 400 μL of buffer A. Excess buffer was blotted off and Alexa Fluor 488-labeled, biotinylated DNA in buffer A was applied to the surface and allowed to bind for 30 min.

5. Remove unbound DNA by blotting and rinsing using three times 400 μL of buffer A.
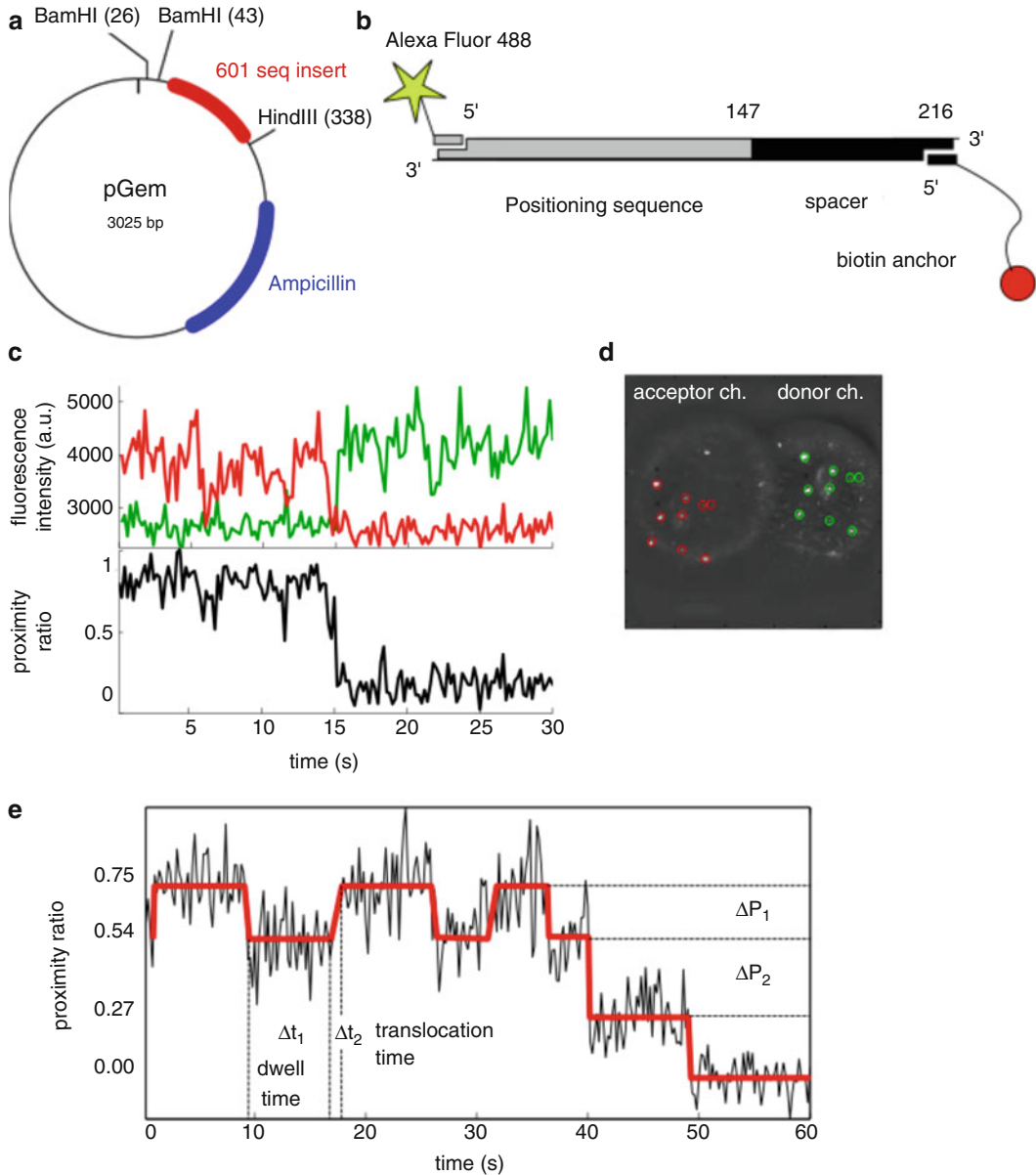
Fig. 4 Preparation of fluorescently labeled and biotinylated dsDNA and TIRF imaging. (**a**) Map of pGEM plasmid with Widom 601 sequence insert. (**b**) Schematics of linear PCR product created with AF488-labeled forward primer and biotinylated reverse primer. (**c**) Time traces of donor (*green*) and acceptor (*red*) and FRET signal (*black*) extracted from corresponding spots in a dual channel image (**d**). (**e**) Time resolved FRET changes observed upon addition of 1 mM ATP

3.11   Single Molecule Imaging

1. In order to avoid photo-destruction samples shall be imaged in anti-photobleaching cocktail: 1.25 mM propyl gallate, 5 mM DTT, 5 mM cysteamine, 1.5 mM β-mercaptoethanol (*see* **Note 43**).

2. Single molecule experiments performed on custom-build TIRFM FRET instrument [34] using imaging rate five frames per second.

3. Optimize protein concentration to minimize background from the bulk-labeled protein while observing enough association with the immobilized DNA (in our case 300 nM).

4. Briefly image immobilized-labeled DNA molecules alone and identify spots (*see* **Note 44**). Only these spots shall be used for further analysis. Image analysis can be done using free software developed by Ha's group: https://cplc.illinois.edu/software/ or simple Matlab scripts.

5. Add labeled protein and image again. Only spatially correlated spots in both channels shall be used (Fig. 4d).

6. Extract time traces and only retain those exhibiting single-step acceptor photobleaching (Fig. 4c).

7. Compute FRET efficiency (proximity ratio) using consecutive single-step acceptor–donor photobleaching sequence [34] or spot intensities corrected for channel sensitivity (Fig. 4c).

8. In steady state, histogram proximity ratios to obtain distributions [34].

9. Add ATP to observe time resolved changes, e.g. bidirectional stepping (Fig. 4e) until all spots photobleach.

4 Notes

1. Primers shall contain appropriate restriction sites for cloning into the desired vector.

2. May need further purifications steps, like ion exchange, to obtain certain proteins.

3. Consider loading concentration and about fivefold dilution on the column to set the sensitivity but the best is to run a test first.

4. Make sure the light scattering is not saturated at the peak maximum.

5. Spin (50 k for 1 h at 4 °C in tabletop ultracentrifuge) to remove as much aggregate as possible.

6. Concentration choice—needs to be high enough for the light-scattering detector to give decent signal while still being within the range.

7. Need to select the right ladder range for the expected length and spacing of putative binding sites, e.g. from less than a nucleosomal repeat (50 bp) to few repeats (1 kb).

8. Select suitable concentration range—usually between high nM to μM—since only relatively stable complexes with dissociation constant $K_d < 0.2$ μM produce discrete shift bands although retardation by transient binding is also possible.

9. NCPs shall be purified first for clean results.

10. The chase experiments are performed to rule out that NCPs are disrupted by CHD4 binding. If disrupted then NCP band would disappear.

11. However, modern instruments, such as GE Healthcare T100, are fully capable of detecting ligand binding in the reverse immobilization format.

12. This is important since K_d derives from the concentration.

13. This is specific for the type of chemistry and to some degree also depends on the vendor.

14. This depends on the instrument sensitivity, while higher density provides higher overall signal, mass transport would certainly be an issue for a large, 100 kDa protein such as CHD4.

15. New instruments have more channels.

16. In order to avoid overcoating this is often done in several steps while observing the R.I. signal.

17. Check flow rate dependence—it should not affect the kinetics. Otherwise there are transport effects and flow rate should be increased.

18. Note that at the beginning of association and dissociation there is an abrupt rise or drop due to so-called bulk contribution from slight buffer mismatch. This is taken into account during data processing.

19. Other nucleotide di/triphosphates and analogues can be used to probe changes in affinity.

20. This is done by scaling the reaction volume down to 200 μL which also saves on consumables having 500 assays instead only 100 per kit.

21. Account for ATP volume if present since it is added last.

22. Use 1:10 dilution of the provided 50 mM stock.

23. Collecting data faster is better but 5 s per well is more than sufficient. This is not an issue for camera-based imaging readers which read all wells at once. However, make sure that the camera-based system can be run in a kinetic mode.

24. Degraded ATP might pose high background and invalidate the assay.

25. This is important if the enzyme is inhibited by P_i—often the rate-limiting step is phosphate release.

26. Note the limits of the coupled reaction, e.g. there is a need to optimize ATPase concentration before doing Michaelis-Menten analysis. V_{max} must be within the rate limit by the coupled PnPase. This rate could be increased by higher PnPase concentration.

27. Similar system has been implemented at Bio-SAXS at Diamond.

28. For shape reconstruction a monodisperse sample is required, best obtained as a fraction from SEC. Some beamlines do have in-line HPLC capability to use with difficult (aggregative) samples.

29. These controls are important to evaluate cleanliness of the flow cell and check for any instrument problems.

30. It is imperative to use the same buffer since even small changes in salt concentration and composition can make subtraction of the baseline difficult or impossible. This is especially important for dilute samples, e.g. protein at or below 1 g/L (w/v) when most of the scattering comes from the solvent/buffer.

31. Now 20×10 s frames are common depending on flux.

32. Radiation damage is manifested by time dependence of the scattering curve and increase in I_0 due to aggregation.

33. However, although the software is smart enough to detect and deal with radiation damage it may not spot other problems. Always check!

34. Guinier plot also useful for extracting the radius of gyration, R_g, and checking for polydispersity (nonlinear Guinier region).

35. Rg for BSA should be ~3 nm, if it is significantly larger or the plot is nonlinear then BSA may be aggregated.

36. Also GASBOR can be used [35] for smaller proteins and takes into account a sequence and medium to wide angle scattering. However, modeling of internal structure is far from reliable.

37. Both fitting procedures should be performed but the latter is computationally intensive and may not yield a unique solution. However, if the data are robust then both solutions are roughly similar, which is reassuring.

38. This can be determined spectrophotometrically by Ellman's reagent or directly from degree of labeling.

39. The final fraction of DMSO needs to be below 5 % to avoid protein aggregation.

40. We chose dialysis instead of LC to prevent further dilution of the sample but in some cases HPLC purification offers advantages of being faster and removing non-specifically attached dye which might leach from the sample later and introduce unwanted background.

41. Protein concentration $= (A_{280} - 0.56\,A_{590})/\varepsilon_M$, where ε_M is the molar extinction coefficient.

42. If the ratio is higher than 3 then labeling with less dye and for a shorter period might decrease the stoichiometry and preferentially label only the most accessible site(s).

43. Degassing all buffers and adding oxygen scavenging (catalase) mix may further prolong the life of the fluorophores.

44. Use shutter to control exposure and limit photobleaching.

Acknowledgements

References

1. Eisen JA, Sweder KS, Hanawalt PC (1995) Evolution of the SNF2 family of proteins: sub-families with distinct sequences and functions. Nucleic Acids Res 23:2715–2723

2. Zhang Y, Ng HH, Erdjument-Bromage H, Tempst P, Bird A, Reinberg D (1999) Analysis of the NuRD subunits reveals a histone deacetylase core complex and a connection with DNA methylation. Genes Dev 13:1924–1935

3. Tong JK, Hassig CA, Schnitzler GR, Kingston RE, Schreiber SL (1998) Chromatin deacetylation by an ATP-dependent nucleosome remodelling complex. Nature 395:917–921

4. Xue Y, Wong J, Moreno GT, Young MK, Cote J, Wang W (1998) NURD, a novel complex with both ATP-dependent chromatin-remodeling and histone deacetylase activities. Mol Cell 2:851–861

5. Feng Q, Zhang Y (2003) The NuRD complex: linking histone modification to nucleosome remodeling. Curr Top Microbiol Immunol 274:269–290

6. Bowen NJ, Fujita N, Kajita M, Wade PA (2004) Mi-2/NuRD: multiple complexes for many purposes. Biochim Biophys Acta 1677:52–57

7. Denslow SA, Wade PA (2007) The human Mi-2/NuRD complex and gene regulation. Oncogene 26:5433–5438

8. Gao H, Lukin K, Ramirez J, Fields S, Lopez D, Hagman J (2009) Opposing effects of SWI/SNF and Mi-2/NuRD chromatin remodeling complexes on epigenetic reprogramming by EBF and Pax5. Proc Natl Acad Sci U S A 106:11258–11263

9. Bienz M (2006) The PHD finger, a nuclear protein-interaction domain. Trends Biochem Sci 31:35–40

10. Shi X, Kachirskaia I, Walter KL, Kuo JH, Lake A, Davrazou F, Chan SM, Martin DG, Fingerman IM, Briggs SD, Howe L, Utz PJ, Kutateladze TG, Lugovskoy AA, Bedford MT, Gozani O (2007) Proteome-wide analysis in Saccharomyces cerevisiae identifies several PHD fingers as novel direct and selective binding modules of histone H3 methylated at either lysine 4 or lysine 36. J Biol Chem 282:2450–2455

11. Pena PV, Davrazou F, Shi X, Walter KL, Verkhusha VV, Gozani O, Zhao R, Kutateladze TG (2006) Molecular mechanism of histone H3K4me3 recognition by plant homeodomain of ING2. Nature 442:100–103

12. Bouazoune K, Mitterweger A, Langst G, Imhof A, Akhtar A, Becker PB, Brehm A (2002) The dMi-2 chromodomains are DNA binding modules important for ATP-dependent nucleosome mobilization. EMBO J 21:2430–2440

13. Akhtar A, Zink D, Becker PB (2000) Chromodomains are protein-RNA interaction modules. Nature 407:405–409

14. Flanagan JF, Mi LZ, Chruszcz M, Cymborowski M, Clines KL, Kim Y, Minor W, Rastinejad F, Khorasanizadeh S (2005) Double chromodomains cooperate to recognize the methylated histone H3 tail. Nature 438:1181–1185

15. Flanagan JF, Blus BJ, Kim D, Clines KL, Rastinejad F, Khorasanizadeh S (2007) Molecular implications of evolutionary differences in CHD double chromodomains. J Mol Biol 369:334–342

16. Marfella CG, Imbalzano AN (2007) The Chd family of chromatin remodelers. Mutat Res 618:30–40

17. Morra R, Lee BM, Shaw H, Tuma R, Mancini EJ (2012) Concerted action of the PHD, chromo and motor domains regulates the human chromatin remodelling ATPase CHD4. FEBS Lett 586:2513–2521

18. Tanaka Y, Tawaramoto-Sasanuma M, Kawaguchi S, Ohta T, Yoda K, Kurumizaka H,

Yokoyama S (2004) Expression and purification of recombinant human histones. Methods 33:3–11

19. Klinker H, Haas C, Harrer N, Becker PB, Mueller-Planitz F (2014) Rapid purification of recombinant histones. PLoS One 9, e104029

20. Dyer PN, Edayathumangalam RS, White CL, Bao Y, Chakravarthy S, Muthurajan UM, Luger K (2004) Reconstitution of nucleosome core particles from recombinant histones and DNA. Methods Enzymol 375:23–44

21. Langst G, Bonte EJ, Corona DF, Becker PB (1999) Nucleosome movement by CHRAC and ISWI without disruption or trans-displacement of the histone octamer. Cell 97:843–852

22. Jonsson U, Fagerstam L, Ivarsson B, Johnsson B, Karlsson R, Lundh K, Lofas S, Persson B, Roos H, Ronnberg I et al (1991) Real-time biospecific interaction analysis using surface plasmon resonance and a sensor chip technology. Biotechniques 11:620–627

23. Lisal J, Tuma R (2005) Cooperative mechanism of RNA packaging motor. J Biol Chem 280:23157–23164

24. Svergun DI, Koch MHJ, Timmins PA, May RP (2013) Small angle X-ray and neutron scattering from solutions of biological macromolecules. International Union of Crystallography Texts on Crystallography, Oxford University Press, Oxford

25. Konarev PV, Volkov VV, Sokolova AV, Koch MHJ, Svergun DI (2003) PRIMUS: a Windows PC-based system for small-angle scattering data analysis. J Appl Crystallogr 36:1277–1282

26. Svergun DI (1991) Mathematical methods in small-angle scattering data analysis. J Appl Crystallogr 24

27. Svergun DI (1992) Determination of the regularization parameter in indirect-transform methods using perceptual criteria. J Appl Crystallogr 25:495–503

28. Svergun DI (1999) Restoring low resolution structure of biological macromolecules from solution scattering using simulated annealing. Biophys J 76:2879–2886

29. Franke D, Svergun DI (2009) DAMMIF, a program for rapid ab-initio shape determination in small-angle scattering. J Appl Crystallogr 42:342–346

30. Kozin MB, Svergun DI (2000) Automated matching of high- and low-resolution structural models. J Appl Crystallogr 34:33–41

31. Volkov VV, Svergun DI (2003) Uniqueness of ab initio shape determination in small-angle scattering. J Appl Crystallogr 36:860–864

32. Pettersen EF, Goddard TD, Huang CC, Couch GS, Greenblatt DM, Meng EC, Ferrin TE (2004) UCSF chimera—a visualization system for exploratory research and analysis. J Comput Chem 25:1605–1612

33. Ha T, Rasnik I, Cheng W, Babcock HP, Gauss GH, Lohman TM, Chu S (2002) Initiation and re-initiation of DNA unwinding by the Escherichia coli Rep helicase. Nature 419:638–641

34. Sharma A, Leach RN, Gell C, Zhang N, Burrows PC, Shepherd DA, Wigneshweraraj S, Smith DA, Zhang X, Buck M, Stockley PG, Tuma R (2014) Domain movements of the enhancer-dependent sigma factor drive DNA delivery into the RNA polymerase active site: insights from single molecule studies. Nucleic Acids Res 42:5177–5190

35. Svergun DI, Petoukhov MV, Koch MHJ (2001) Determination of domain structure of proteins from X-ray solution scattering. Biophys J 80:2946–2953